# Concurrent validation of the Xsens IMU system of lower-body kinematics in jump-landing and change-of-direction tasks

Nijmeijer, Eline M.; Heuvelmans, Pieter; Bolt, Ruben; Gokeler, Alli; Otten, Egbert; Benjaminse, Anne

*Published in:*
Journal of biomechanics

*DOI:*
10.1016/j.jbiomech.2023.111637

Journal of Biomechanics 154 (2023) 111637

Contents lists available at ScienceDirect

Journal of Biomechanics

journal homepage: www.elsevier.com/locate/jbiomech

# Concurrent validation of the Xsens IMU system of lower-body kinematics in jump-landing and change-of-direction tasks

Eline M. Nijmeijer [a], Pieter Heuvelmans [b], Ruben Bolt [a], Alli Gokeler [b,c,d], Egbert Otten [a], Anne Benjaminse [a,e,*]

[a] Department of Human Movement Sciences, University Medical Center Groningen, University of Groningen, The Netherlands
[b] Exercise Science and Neuroscience Unit, Department of Exercise & Health, Paderborn University, Germany
[c] Amsterdam Collaboration for Health and Safety in Sports, Department of Public and Occupational Health, Amsterdam Movement Sciences, VU University Medical Center Amsterdam, the Netherlands
[d] Faculty of Health, Amsterdam University of Applied Sciences, Amsterdam, The Netherlands
[e] School of Sport Studies, Hanze University Groningen, The Netherlands

ARTICLE INFO

*Keywords:*
Inertial measurement units
Optoelectronic motion system
Validation
Jump-landing
Change-of-direction

ABSTRACT

Inertial measurement units (IMUs) allow for measurements of kinematic movements outside the laboratory, persevering the athlete-environment relationship. To use IMUs in a sport-specific setting, it is necessary to validate sport-specific movements. The aim of this study was to assess the concurrent validity of the Xsens IMU system by comparing it to the Vicon optoelectronic motion system for lower-limb joint angle measurements during jump-landing and change-of-direction tasks. Ten recreational athletes performed four tasks; single-leg hop and landing, running double-leg vertical jump landing, single-leg deceleration and push off, and sidestep cut, while kinematics were recorded by 17 IMUs (Xsens Technologies B.V.) and eight motion capture cameras (Vicon Motion Systems, Ltd). Validity of lower-body joint kinematics was assessed using measures of agreement (cross-correlation: XCORR) and error (root mean square deviation and amplitude difference). Excellent agreement was found in the sagittal plane for all joints and tasks (XCORR > 0.92). Highly variable agreement was found for knee and ankle in transverse and frontal plane. Relatively high error rates were found in all joints. In conclusion, this study shows that the Xsens IMU system provides highly comparable waveforms of sagittal lower-body joint kinematics in sport-specific movements. Caution is advised interpreting frontal and transverse plane kinematics as between-system agreement highly varied.

## 1. Introduction

Optoelectronic motion capture (OMC) systems, such as Vicon (Windolf et al., 2008), provide accurate measurements of kinematics in the laboratory (McGinley et al., 2009). Small capture area and visual obstructions (i.e., other players and body segments) are drawbacks of these systems. Recent research showed that movement patterns in the laboratory and field differ (Di Paolo et al., 2022, Di Paolo et al., 2023) and amplify the need to examine movement patterns in ecological environments to better understand injury risk and performance (Bolt et al., 2021). The use of inertial measurement units (IMUs) allows for measurements in sport-specific contexts (Bolt et al., 2021).

There is a need to validate IMUs while performing fast, dynamic movements, such as accelerations and decelerations. Therefore, the aim of this study is to assess the concurrent validity of the Xsens IMU system by comparing it to the Vicon OMC system for lower-limb joint angle measurements during jump-landing and change-of-direction tasks. Based on previous studies, high concurrent validity of sagittal angles was hypothesized (Al-Amri et al., 2018; Zhang et al., 2013).

## 2. Materials and methods

Ten recreational athletes, five females and five males (age: 20.2 ± 1.4; 24.2 ± 2.2 yrs, height: 171.6 ± 8.3; 184.8 ± 7.1 cm, mass: 62.1 ± 8.3; 79.3 ± 11.1 kg) were included. Participants signed Informed consent and ethical approval was obtained from the (*Blinded for submission*)

* Corresponding author at: Department of Human Movement Sciences, Faculty of Medical Sciences, University of Groningen, Antonius Deusinglaan 1, 9713 AV, Groningen, The Netherlands.
*E-mail address:* a.benjaminse@umcg.nl (A. Benjaminse).

https://doi.org/10.1016/j.jbiomech.2023.111637
Accepted 10 May 2023
Available online 15 May 2023

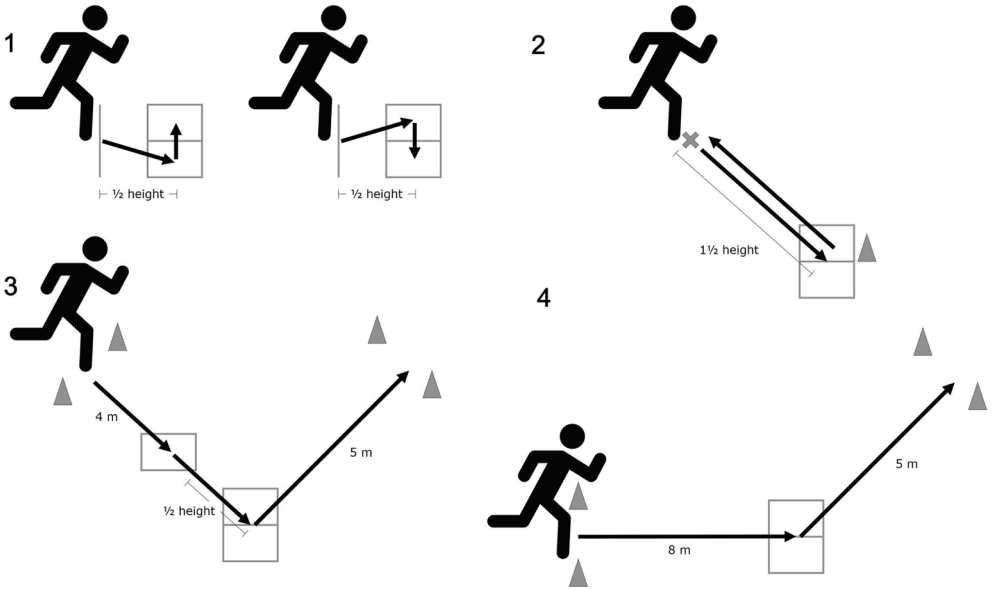


**Fig. 1.** Change-of-direction and jump-landing tasks for right-leg dominance. 1) single-leg hop and landing (SLH): participants performed a single-leg hop to the ipsilateral target with their dominant leg, immediately followed by a single-leg hop to the contralateral target, or vice versa, 2) running double-leg vertical jump landing (DVJH): participants ran towards the targets at 45-degree angle. After pushing off with their non-dominant leg, participants performed a double-leg landing on the targets, immediately followed by a double-leg vertical jump. After the second landing, the participants shuffled in a perpendicular direction for 5 m, contralateral to their dominant leg, 3) single-leg deceleration and push-off (SLD): participants performed quick steps towards the targets at 45-degree angle. Upon landing on the target with their dominant leg, the participants performed a single-leg deceleration and push-off to return to their starting position, 4) running sidestep cut (SSC): participants ran at a submaximal speed 5 m towards the targets and performed a 45-degree sidestep cut with their dominant leg on the target and continued running for 5 m. The distances of hopping and jumping were scaled to the participants height.

(IRB nr. *Blinded for submission*).

### 2.1. Instruments and procedures

Participants wore a MVN lycra suit (MVN Link BIOMECH full body, Xsens, Enschede, the Netherlands), containing 17 IMUs, a battery pack (95 × 59 × 25mm:70 g) and a transponder (160 × 72 × 25mm:150 g). Each IMU (36 × 24 × 10mm:10 g) integrates a 3D accelerometer (scale: ±160 m/s$^2$, noise: 0.003 m/s$^2$/$\sqrt{}$Hz), 3D gyroscope (±2000°/s, 0.05°/s/$\sqrt{}$Hz) and 3D magnetometer (±1.9 Gauss, 0.15 m Gauss/$\sqrt{}$Hz), internally sampling at 1000 Hz. The sample rate of the Xsens system is 240 Hz (Schepers et al., 2018). Anthropometric measurements and IMU placement were done according to the manufacturer's recommendations (Schepers et al., 2018).

Sixteen reflective markers were placed on the suit according to the Vicon Plug-in Gait (PiG) model (Appendix Fig. A1). Five reflective markers were placed on sternum, clavicle, C7, T10, and right scapula for the trunk model (Nijmeijer et al., 2022). Anthropometric data were entered into the PiG model. High test and retest repeatability and good measurement accuracy of this model in sagittal kinematics have been reported (Kadaba et al., 1989; McGinley et al., 2009). Eight Vicon T10 cameras (Vicon Motion Systems Ltd, Oxford, UK) captured lower body kinematics at 100 Hz. Participants moved in a laboratory with a measuring volume of 180 m$^3$. A N-pose + walk (Xsens) and T-pose (Vicon) calibration were performed according to the manufacturer's recommendation (Vicon Motion Systems, 2016; Xsens Technologies, 2021).

### 2.2. Tasks

Participants performed four tasks; 1) single-leg hop (SLH), 2) running double-leg vertical jump (DLVJ), 3) single-leg deceleration and push-off (SLD) and, 4) running sidestep cut (SSC) as reported in detail previously. The SLH, DLVJ, and SLD were personalized based on body height (Heuvelmans et al., 2022) (Fig. 1). Leg dominance was defined as the preferred leg for jumping and landing (Heuvelmans et al., 2022). After warming up and task demonstration, the participant used familiarization trials at his own discretion. Thereafter, participants performed five successful trials for each task. In addition, participants were encouraged to run and cut at submaximal speed (task 2–4) and coached when they deviated from this. A 30 s rest-period was applied between trials. Trials were assessed and discarded if the participant lost balance. Participants were measured in two sessions with a 5–7 day interval.

### 2.3. Data processing

Raw motion analysis data were digitized in Nexus (2.7.1, Vicon Motion Systems Ltd, Oxford, UK) and Xsens MVN Analyze (2019.2.1). A fourth-order zero lag Butterworth low-pass filter at 10 Hz was used to filter the Vicon data (Benjaminse et al., 2017). Modeling procedures for IMU data were based on the manufacturer's recommendations (Schepers et al., 2018). Sensor fusion for IMU data was performed using the proprietary algorithms (Xsens Kalman Filter) and filtered using the LXsolver (minimize soft tissue artefact) in MVN Biomech Studio. Further data processing and waveform analyses were conducted with customized software using MATLAB 9.6 (The MathWorks Inc., Natick, MA). Raw Xsens quaternion data were matched with Vicon conventions as follows. Xsens quaternions were transferred to Euler angles in degrees through a rotation matrix. The Vicon Euler angle order of YXZ for hip, knee and ankle joints and their signs (+/−) were taken as the convention, i.e., medial–lateral, anterior-posterior and axial directions. Data of both systems were synchronized, and time matched through cross-correlations of joint angles with the highest amplitudes. Entire trials were analyzed including swing phase, stand phase and swing phase of both legs. Outlying data were regarded as part of the observations and therefore only excluded if no comparison could be made between systems due to technical issues.

### 2.4. Statistical analyses

Frontal (abduction/adduction), sagittal (flexion/extension) and transverse (axial rotation) kinematics of hip, knee and ankle were analyzed. Cross-correlation (XCORR), root mean square deviation (RMSD), and amplitude difference (ΔAMP) were assessed. Level of agreement between time series was interpreted as 'poor' (XCORR $<$ 0.40), 'fair' (0.40 $\leq$ XCORR $<$ 0.75), and 'excellent' (XCORR $\geq$ 0.75) (Duffell et al., 2014). RMSD and ΔAMP (Xsens minus Vicon) are measures of disagreement and were calculated as done previously

**Table 1**
Measures of agreement (XCORR), and disagreement (RMSD, ΔAMP) between the two motion capture systems for the four tasks, median (interquartile range) of the dominant leg.lv.

| | Hip | | | Knee | | | Ankle | | |
|---|---|---|---|---|---|---|---|---|---|
| | Sagittal | Frontal | Transverse | Sagittal | Frontal | Transverse | Sagittal | Frontal | Transverse |
| XCORR | | | | | | | | | |
| SLH | 0.96 (0.08) | 0.69 (0.50) | 0.58 (0.81) | 0.96 (0.08) | 0.32 (0.30) | 0.26 (0.26) | 0.92 (0.16) | 0.47 (0.53) | 0.32 (0.68) |
| DLVJ | 0.99 (0.02) | 0.98 (0.06) | 0.79 (0.63) | 0.99 (0.00) | 0.36 (0.20) | 0.17 (0.26) | 0.99 (0.01) | 0.04 (0.17) | 0.41 (0.59) |
| SLD | 0.99 (0.01) | 0.99 (0.05) | 0.62 (0.44) | 0.99 (0.01) | 0.15 (0.46) | 0.22 (0.35) | 0.97 (0.05) | 0.00 (0.11) | 0.53 (0.80) |
| SSC | 0.96 (0.06) | 0.87 (0.75) | 0.63 (0.41) | 0.98 (0.04) | 0.47 (0.36) | 0.39 (0.39) | 0.95 (0.12) | 0.01 (0.45) | 0.58 (0.62) |
| All tasks | 0.98 (0.05) | 0.89 (0.50) | 0.66 (0.61) | 0.99 (0.05) | 0.34 (0.32) | 0.26 (0.32) | 0.96 (0.05) | 0.12 (0.54) | 0.43 (0.68) |
| RMSD | | | | | | | | | |
| SLH | 17.46 (10.88) | 8.16 (4.84) | 8.45 (7.75) | 16.41 (10.16) | 6.13 (3.57) | 12.12 (8.45) | 13.09 (10.34) | 7.26 (4.08) | 15.18 (9.41) |
| DLVJ | 14.95 (8.55) | 6.79 (5.47) | 9.53 (7.22) | 5.74 (4.22) | 8.63 (3.71) | 11.78 (7.64) | 5.93 (1.44) | 11.82 (4.56) | 11.89 (9.60) |
| SLD | 13.34 (9.67) | 7.62 (8.11) | 7.82 (4.77) | 7.71 (5.73) | 10.24 (10.29) | 13.01 (8.65) | 5.23 (2.40) | 12.21 (6.95) | 15.89 (12.73) |
| SSC | 13.16 (8.26) | 9.35 (11.05) | 9.60 (8.15) | 15.00 (14.95) | 6.87 (3.09) | 12.63 (8.17) | 8.07 (6.21) | 12.70 (5.36) | 12.42 (9.91) |
| All tasks | 15.31 (9.85) | 7.92 (6.89) | 8.56 (7.36) | 11.33 (12.60) | 7.52 (4.69) | 12.22 (8.30) | 7.41 (7.97) | 10.40 (6.14) | 14.24 (10.60) |
| All tasks - as % of ROM | 10.6[a] | 8.8[a] | 9.5[b] | 8.1[a] | 75.2[c] | 17.5[d] | 10.6[e] | 28.9[e] | 19.5[e] |
| ΔAMP | | | | | | | | | |
| SLH | −7.35 (6.57) | −3.47 (4.95) | −4.00 (9.26) | 1.91 (4.70) | −2.49 (5.48) | −4.89 (6.78) | 9.90 (7.33) | 16.99 (9.65) | −8.10 (9.35) |
| DLVJ | −8.49 (11.42) | −4.04 (4.72) | −2.11 (9.23) | −0.23 (6.10) | −2.46 (6.98) | −4.88 (9.18) | 13.70 (7.84) | 17.23 (6.64) | −3.21 (7.54) |
| SLD | 0.12 (7.77) | −3.14 (4.21) | −3.50 (8.92) | 3.87 (5.23) | −4.85 (7.89) | −9.73 (11.46) | 7.63 (7.82) | 13.65 (6.83) | −4.02 (11.02) |
| SSC | −13.58 (8.15) | −2.15 (7.79) | −7.97 (8.86) | −0.38 (16.43) | −4.38 (7.36) | −4.33 (8.37) | 8.23 (9.80) | 12.81 (9.89) | −5.81 (10.74) |
| All tasks | −7.61 (11.16) | −3.46 (4.98) | −4.30 (9.57) | 1.59 (6.89) | −3.34 (6.83) | −5.22 (8.98) | 9.87 (9.49) | 15.99 (7.89) | −5.74 (9.41) |

XCORR = cross-correlation; RMSD = root mean square deviation; ΔAMP = amplitude difference; SLH = single-leg hop; DLVJ = running double-leg vertical jump; SLD = single-leg deceleration and push-off; SSC = running sidestep cut. References for range of motion values.
[a] Roach & Miles (1991).
[b] Han et al. (2015).
[c] Reinschmidt et al. (1997).
[d] Zarins et al. (1983).
[e] Grimston et al. (1993).

(Heuvelmans et al., 2022). To provide more insight, RMSD values were normalized to earlier published joint's range of motion (ROM). Level of disagreement was interpreted as 'low' if the value was $\leq 5^\circ$ (Di Paolo et al., 2021). As the tasks were mainly eliciting movement of the dominant leg, results of this leg are reported and discussed in text. Results of the non-dominant leg are presented in the Appendix (Table A1 and Fig. A2).

## 3. Results

A total of 480 trials (96 %) were included and used for comparison between the two systems. Twenty trials (12 SLH, 1 DLVJ, 7 SLD) were excluded from further analysis due to failure of one of the systems to record the full trial. Exact values of XCORR, RMSD and ΔAMP are provided in Table 1.

### 3.1. Agreement

Sagittal joint angles demonstrated excellent XCORR for all joints (median $\geq$ 0.96, IQR: 0.05). Frontal joint angles presented excellent XCORR for hip (median: 0.89, IQR: 0.50), but poor XCORR for knee (median: 0.34, IQR: 0.32) and ankle (median: 0.12, IQR: 0.54). XCORR of the transverse angles were fair for hip (median: 0.66, IQR: 0.61) and ankle (median: 0.43, IQR: 0.68), but poor for knee (median: 0.26, IQR: 0.32).

### 3.2. Disagreement

Knee frontal angles had the highest relative RMSD (median: 7.5° (75 % ROM), IQR: 4.7°), followed by ankle frontal (median: 10.4° (29 % ROM), IQR: 6.1°) and transverse (median: 14.2° (20 % ROM), IQR: 10.6°) angles. Knee sagittal (median: 11.3° (8 % ROM), IQR: 12.6°) and hip frontal (median: 7.9° (9 % ROM), IQR: 6.9°) angles showed the lowest relative RMSD. Ankle frontal angles (median: 16.0°, IQR: 7.9°) demonstrated the highest ΔAMP followed by ankle (median: 9.9°, IQR: 9.5°) and hip sagittal (median: −7.6°, IQR: 11.2°) angles (Fig. 2).

### 3.3. Tasks

All tasks displayed excellent XCORR for sagittal joint angles. XCORR was excellent for hip frontal angles, except for SLH. Fair XCORR was found for hip transverse angles, except for DLVJ. Poor XCORR for knee frontal and transverse angles were found, except for knee frontal angle in SSC which was fair. Ankle frontal and transverse joint angles showed poor to fair XCORR in all tasks. SLH featured the highest RMSD for sagittal plane joint angles. The other RMSDs ranged from 5.2° to 15.9° across tasks and joint angles. All tasks demonstrated high ΔAMP for ankle sagittal and frontal angles. Low ΔAMP were found for the knee in all planes, except for the transverse plane in SLD. The other ΔAMPs ranged from 0.1° to −13.6° across tasks and joint angles.

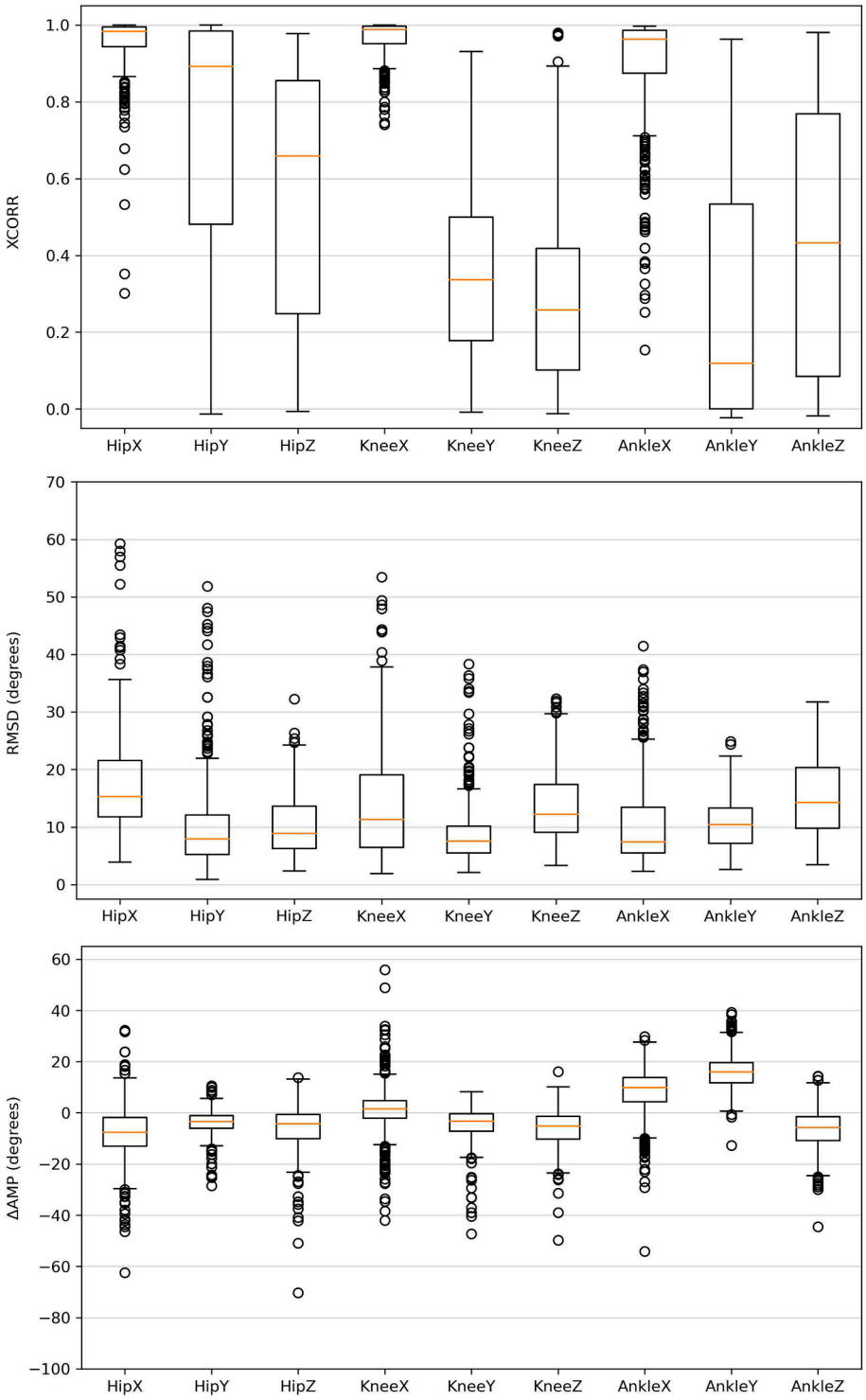


**Fig. 2.** Cross-correlations (XCORR) (top), root mean square deviations (RMSD) (middle) and amplitude differences (ΔAMP) (bottom) between the two motion capture systems of the dominant leg. The X, Y and Z correspond to flexion/extension, abduction/adduction and axial rotation angles respectively (i.e. HipX refers to Hip flexion/extension angle).

## 4. Discussion

The results showed that the two systems had high agreement for the sagittal plane and frontal hip angles. Poor to fair agreement was found in the transverse and frontal plane for the knee and ankle joint, replicating previous studies comparing OMC systems and IMUs for dynamic movements (Di Paolo et al., 2021; Heuvelmans et al., 2022). It is important to note that the used PiG model has shown good repeatability and accuracy for the sagittal plane, however performs suboptimal in the other planes (Duffell et al., 2014; Sinclair et al., 2015). Therefore, caution should be taken when interpreting the results of these planes.

The high cross-correlation values indicates that sagittal joint angle waveforms from Xsens were similar to those from Vicon. The high agreement in the jumping tasks confirms the suggestion that jumping does not adversely affect the sagittal kinematics provided by Xsens (Al-Amri et al., 2018). Interestingly, low XCORR values were found for the

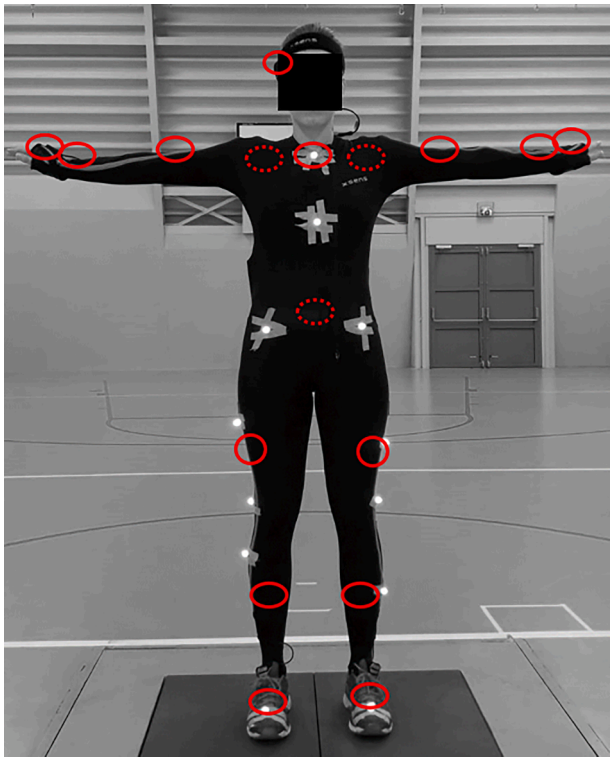

**Fig. A1.** Placements of reflective markers (Vicon) and inertial measurement units (Xsens) marked with red circles (frontal view), inertial measurement units (Xsens) at the dorsal side are marked with dotted red circles.

frontal ankle. Fair agreement was found in the SLH, whereas extremely poor agreement was found in the other tasks, which could indeed be regarded as more dynamic and faster. Previous research also found lower agreement in jumping compared to squatting regarding frontal ankle angle (Al-Amri et al., 2018). Moreover, lower agreement rates were found investigating kicking biomechanics at high speeds compared to lower speed movements (Blair et al., 2018), thus confirming less agreement in the more dynamic, fast tasks (Poitras et al., 2019).

Large disagreements in joint angles between the systems were particularly noticeable for frontal and transverse knee and ankle angles. This is in line with previous studies showing large differences for ankle transverse angle (Al-Amri et al., 2018; Heuvelmans et al., 2022) and transverse knee angle comparing IMUs to Vicon PiG data (Al-Amri et al., 2018). Our data showed a knee transverse angle difference of 12.2°, which is still large for a joint with relatively small range of motion in the transverse plane (17.5 % of ROM).

The highest amplitude differences were found for ankle frontal and sagittal angle. This amplifies the heightened amount of disagreement when progressing to more dynamic tasks as also found previously (Heuvelmans et al., 2022; Teufl et al., 2019). Conversely, low amplitude differences were found for the knee in all planes. This is even more interesting because the cross-correlation values of the knee frontal and transverse angle were poor. So, despite the small absolute differences reported at discrete time points, large differences were seen comparing the waveforms of the systems regarding these planes of the knee. This so-called phenomenon crosstalk refers to significant errors in frontal and transverse angle curves due to minor changes of marker placements (Piazza & Cavanagh, 2000). Therefore, it could not be said with certainty that disagreements between Vicon and Xsens are caused by the same system all the time and one system is inferior or superior to the other, as Vicon may have flaws as well (i.e., wobbling of muscle mass). In our data, we have seen examples in which the knee frontal and transverse angle of Vicon deviates from Xsens whereas the sagittal angle of Vicon and Xsens goes in synchronization (Fig. A3). This may explain the small RMSD and ΔAMP differences whereas the waveforms show less agreement. Fortunately, there are methods to correct for this phenomenon (Baudet et al., 2014).

Additional analysis was performed to investigate the outliers in our data. There was a substantial number of outliers of XCORR (n = 118 divided amongst 9 variables and 480 trials) present in the sagittal plane which was also seen previously (Heuvelmans et al., 2022). This may be due to high median XCORR values (≥0.96) and low IQR (0.05) which logically results in a large area of values classified as outliers. On the contrary, although the high median XCORR of the hip frontal plane (0.89), the IQR was also high (0.50) which reduces the area in which outliers could be present, indicating a large spread of values. This should be considered when interpreting the obtained values. After intensive training by a senior researcher, one researcher fixated all sensors and markers during both sessions which maximized the intrareliability regarding sensor placement. Moreover, as all tasks were performed in direct succession and no markers were reattached, the change of unequal distribution of outliers amongst the tasks is low. Lastly, the distribution of outliers over the trial numbers did not differ substantially. Fig. 2 showed a substantial amount of outliers present in RMSD and ΔAMP data highlighting the assumption that it is unclear if Xsens or Vicon does overestimate the other system and they cannot be used interchangeably.

This study contributes to emerging evidence pertaining to the validity of IMUs during dynamic tasks (Al-Amri et al., 2018; Poitras et al., 2019; Zhang et al., 2013) and incorporating lower-body kinematics in all planes (Di Paolo et al., 2021; Heuvelmans et al., 2022). The IMUs were able to provide valid estimates for sagittal kinematics, but less satisfactory results regarding transversal and frontal kinematics. This provides opportunities for future research and implies that IMUs could be used to measure lower-body sagittal kinematics in sport-specific situations on field. Secondly, our results indicate that regardless of waveform agreement, offset errors between Vicon and Xsens did exist. This confirms previous findings of over- or underestimating kinematics (Teufl et al., 2019). A between-system discrepancy in setting the 0° point for joints through calibration may explain this (Heuvelmans et al., 2022). This should be considered when kinematics are used and decisions are made based on known cut-off values. Moreover, the systems cannot be used interchangeably without correction methods to correct for these offset errors.

A limitation of this study is the Vicon marker set used (PiG). Higher disagreement values validating IMUs with single compared to cluster markers advocates the use of cluster markers (Teufl et al., 2019). Moreover, a set-up with more markers (i.e., full body PiG model) could have led to higher accuracy. However, the PiG model was chosen for the current study as it is a frequently applied set-up in this type of research (Benjaminse et al., 2017; Heuvelmans et al., 2022), designed for practical applications due to its simplicity and used previously to validate IMUs which makes direct comparisons to these studies possible (Al-Amri et al., 2018; Heuvelmans et al., 2022). Secondly, the systems' comparison was based on kinematics only. This is a limitation of wearable technology compared to OMC systems. Current injury risk screening is based on kinematics and kinetics (Robinson et al., 2023). Nevertheless, with the gained knowledge, we are closer to performing injury risk screening in ecological valid environments instead of the laboratory (e.g. (Leppänen et al., 2017)). For example, sagittal hip and knee kinematics could be used to provide information about shock absorption during cutting or jumping as is done recently to examine if injury risk factors in lab reflect injury risk on field (Di Paolo et al., 2023). Further studies should examine the appropriate sets of wearable sensors, musculoskeletal modeling steps and artificial intelligence models to estimate kinetics on field which could provide even more, necessary information for injury risk screening (Lloyd, 2021).

In conclusion, this study shows that the Xsens IMU system can provide highly comparable waveforms of sagittal lower-body kinematics during jump-landing and change-of-direction tasks compared to the

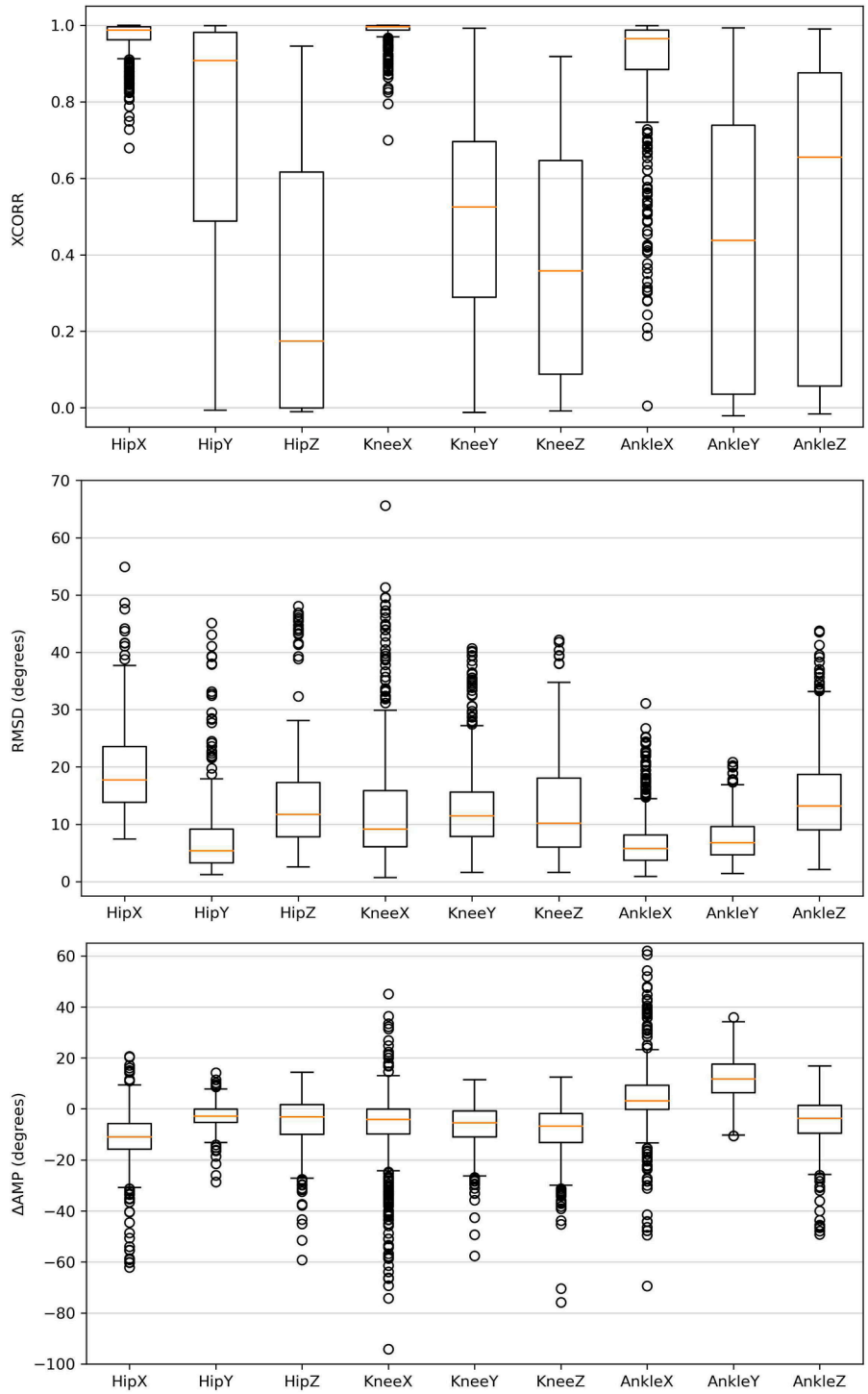


**Fig. A2.** Cross-correlations (XCORR) (top), root mean square deviations (RMSD) (middle) and amplitude differences (ΔAMP) (bottom) between the two motion capture systems of the non-dominant leg. The X, Y and Z correspond to flexion/extension, abduction/adduction and axial rotation angles respectively (i.e. HipX refers to Hip flexion/extension angle).

Vicon OMC system. This is promising for on field research to gain more knowledge about movement patterns in an ecological environment. However, the systems cannot be used interchangeably, as high amplitude differences and deviations were found for sagittal angles. Caution should be taken when interpreting frontal and transverse kinematics as between-system agreement is highly variable.

## Funding

The authors reported there is no funding associated with the work featured in this article.

## CRediT authorship contribution statement

**Eline M. Nijmeijer:** Writing – original draft, Visualization. **Pieter**

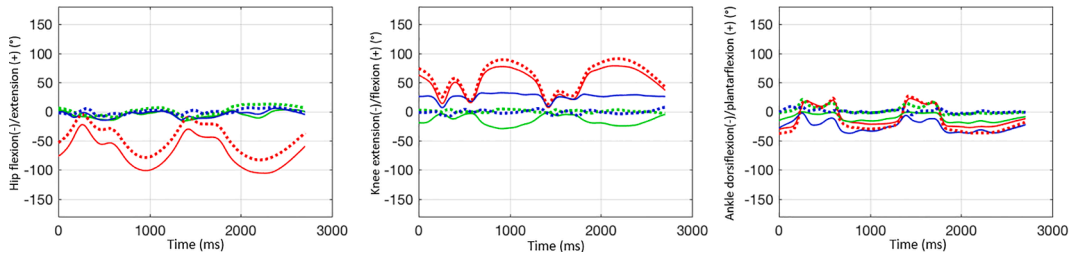


**Fig. A3.** Example of cross-talk of the frontal and transverse joint angles calculated with the Vicon (solid lines) and Xsens (dotted lines) system. Red, green and blue lines correspond to sagittal, frontal and transverse plane respectively.

**Heuvelmans:** Writing – review & editing, Visualization, Validation, Methodology, Investigation, Formal analysis, Data curation, Conceptualization. **Ruben Bolt:** Writing – review & editing, Visualization, Validation, Methodology, Investigation, Formal analysis, Data curation, Conceptualization. **Alli Gokeler:** Writing – review & editing, Visualization, Validation, Supervision, Resources, Project administration, Methodology, Investigation, Conceptualization. **Egbert Otten:** Writing – review & editing, Software, Formal analysis, Data curation. **Anne Benjaminse:** Writing – review & editing, Visualization, Validation, Supervision, Resources, Project administration, Methodology, Investigation, Conceptualization.

## Declaration of Competing Interest

The authors declare that they have no known competing financial interests or personal relationships that could have appeared to influence the work reported in this paper.

## Acknowledgments

None. The authors did not make use of writing assistance.

## Appendix A

**Table A1**
Measures of agreement (XCORR), and disagreement (RMSD, ΔAMP) between the two motion capture systems for the four tasks, median (interquartile range) of the non dominant leg.

| | Hip | | | Knee | | | Ankle | | |
|---|---|---|---|---|---|---|---|---|---|
| | Sagittal | Frontal | Transverse | Sagittal | Frontal | Transverse | Sagittal | Frontal | Transverse |
| XCORR | | | | | | | | | |
| SLH | 0.97 (0.06) | 0.88 (0.37) | 0.09 (0.55) | 0.99 (0.01) | 0.49 (0.42) | 0.25 (0.70) | 0.96 (0.10) | 0.38 (0.76) | 0.60 (0.90) |
| DLVJ | 0.99 (0.01) | 0.98 (0.09) | 0.22 (0.58) | 0.99 (0.00) | 0.52 (0.33) | 0.33 (0.44) | 0.98 (0.02) | 0.49 (0.52) | 0.55 (0.72) |
| SLD | 0.99 (0.02) | 0.99 (0.05) | 0.07 (0.53) | 0.99 (0.00) | 0.56 (0.50) | 0.41 (0.50) | 0.97 (0.06) | 0.54 (0.74) | 0.78 (0.71) |
| SSC | 0.99 (0.03) | 0.61 (0.60) | 0.36 (0.71) | 0.99 (0.02) | 0.54 (0.36) | 0.53 (0.50) | 0.88 (0.27) | 0.31 (0.70) | 0.68 (0.62) |
| All tasks | 0.99 (0.03) | 0.91 (0.49) | 0.17 (0.62) | 0.99 (0.01) | 0.53 (0.41) | 0.36 (0.56) | 0.96 (0.10) | 0.44 (0.71) | 0.66 (0.82) |
| RMSD | | | | | | | | | |
| SLH | 17.15 (11.69) | 6.47 (4.39) | 11.65 (9.44) | 12.64 (10.99) | 10.49 (8.90) | 9.64 (12.48) | 5.44 (3.89) | 5.96 \(4.06) | 12.24 (12.77) |
| DLVJ | 16.58 (6.93) | 3.65 (7.30) | 11.73 (8.51) | 6.45 (4.71) | 10.95 (3.82) | 11.37 (11.68) | 5.96 (2.41) | 9.09 (3.57) | 13.24 (7.49) |
| SLD | 19.88 (8.53) | 4.16 (6.37) | 12.79 (10.64) | 6.46 (3.31) | 11.78 (6.21) | 9.68 (13.52) | 4.42 (4.01) | 5.60 (4.09) | 12.73 (9.36) |
| SSC | 18.51 (8.98) | 5.83 (5.82) | 10.87 (9.67) | 12.50 (9.76) | 13.25 (12.29) | 9.91 (9.80) | 7.96 (8.11) | 7.83 (4.57) | 14.91 (9.11) |
| All tasks | 17.75 (9.78) | 5.38 (5.90) | 11.73 (9.53) | 9.13 (9.84) | 11.44 (7.79) | 10.20 (12.07) | 5.74 (4.44) | 6.79 (4.97) | 13.16 (9.72) |
| All tasks - as % of ROM | 12.3[a] | 6.0[a] | 13.0[b] | 6.5[a] | 114.4[c] | 14.6[d] | 8.2[e] | 18.9[e] | 18.0[e] |
| ΔAMP | | | | | | | | | |
| SLH | −10.09 (9.15) | −3.39 (4.58) | 1.02 (7.50) | −6.59 (11.86) | −4.06 (6.61) | −5.50 (8.54) | 1.49 (4.42) | 8.000 (7.52) | −1.86 (8.27) |
| DLVJ | −11.38 (11.23) | −280 (4.96) | −6.95 (14.86) | −1.21 (6.14) | −2.21 (19.98) | −8.96 (15.82) | 9.32 (11.08) | 20.37 (7.18) | −3.98 (9.97) |
| SLD | −6.47 (8.37) | −0.83 (5.21) | −3.18(8.36) | −4.25 (7.04) | −3.50 (10.89) | −3.16 (12.17) | 3.33 (8.64) | 10.85 (7.85) | −5.09 (12.28) |
| SSC | −15.36 (10.45) | −3.81 (5.45) | −6.67 (9.87) | −6.52 (25.13) | −12.46 (10.42) | −10.62 (10.34) | 5.8 (19.58) | 13.62 (13.76) | −7.67 (13.93) |
| All tasks | −11.01 (10.19) | −2.83 (5.34) | −3.15 (11.62) | −4.12 (9.74) | −5.48 (10.29) | −6.72 (11.35) | 3.06 (9.44) | 11.76 (11.27) | −3.70 (11.00) |

XCORR = cross-correlation; RMSD = root mean square deviation; ΔAMP = amplitude difference; SLH = single-leg hop; DLVJ = running double-leg vertical jump; SLD = single-leg deceleration and push-off; SSC = running sidestep cut. References for range of motion values;

[a] Roach & Miles (1991).
[b] Han et al. (2015).
[c] Reinschmidt et al. (1997).
[d] Zarins et al. (1983).
[e] Grimston et al. (1993).

## References


Al-Amri, M., Nicholas, K., Button, K., Sparkes, V., Sheeran, L., Davies, J., 2018. Inertial measurement units for clinical movement analysis: Reliability and concurrent validity. Sensors 18 (3), 719. https://doi.org/10.3390/s18030719.

Baudet, A., Morisset, C., d'Athis, P., Maillefert, J.-F., Casillas, J.-M., Ornetti, P., Laroche, D., Fasano, A., 2014. Cross-talk correction method for knee kinematics in gait analysis using principal component analysis (PCA): A new proposal. PLoS One 9 (7), e102098.

Benjaminse, A., Otten, B., Gokeler, A., Diercks, R.L., Lemmink, K.A.P.M., 2017. Motor learning strategies in basketball players and its implications for ACL injury prevention: A randomized controlled trial. Knee Surgery Sports Traumatol. Arthrosc. 25 (8), 2365–2376. https://doi.org/10.1007/s00167-015-3727-0.

Blair, S., Duthie, G., Robertson, S., Hopkins, W., Ball, K., 2018. Concurrent validation of an inertial measurement system to quantify kicking biomechanics in four football codes. J. Biomech. 73, 24–32. https://doi.org/10.1016/j.jbiomech.2018.03.031.

Bolt, R., Heuvelmans, P., Benjaminse, A., Robinson, M.A., Gokeler, A., 2021. An ecological dynamics approach to ACL injury risk research: A current opinion. Sports Biomech. 1–14 https://doi.org/10.1080/14763141.2021.1960419.

Di Paolo, S., Nijmeijer, E.M., Bragonzoni, L., Gokeler, A., Benjaminse, A., 2023. Definition of High-Risk Motion Patterns for Female ACL Injury Based on Football-Specific Field Data: A Wearable Sensors Plus Data Mining Approach. Sensors 23 (4), 2176. https://doi.org/10.3390/s23042176.

Di Paolo, S., Lopomo, N.F., Della Villa, F., Paolini, G., Figari, G., Bragonzoni, L., Grassi, A., Zaffagnini, S., 2021. Rehabilitation and return to sport assessment after anterior cruciate ligament injury: quantifying joint kinematics during complex high-speed tasks through wearable sensors. Sensors 21 (7), 2331. https://doi.org/10.3390/s21072331.

Di Paolo, S., Nijmeijer, E., Bragonzoni, L., Dingshoff, E., Gokeler, A., Benjaminse, A., 2022. Comparing lab and field agility kinematics in young talented female football players: Implications for ACL injury prevention. Eur. J. Sport Sci. 1–10 https://doi.org/10.1080/17461391.2022.2064771.

Duffell, L.D., Hope, N., McGregor, A.H., 2014. Comparison of kinematic and kinetic parameters calculated using a cluster-based model and Vicon's plug-in gait. Proc. Inst. Mech. Eng. 228 (2), 206–210. https://doi.org/10.1177/0954411913518747.

Grimston, S.K., Nigg, B.M., Hanley, D.A., Engsberg, J.R., 1993. Differences in Ankle joint complex range of motion as a function of age. Foot Ankle 14 (4), 215–222. https://doi.org/10.1177/107110079301400407.

Han, H., Kubo, A., Kurosawa, K., Maruichi, S., Maruyama, H., 2015. Hip rotation range of motion in sitting and prone positions in healthy Japanese adults. J. Phys. Ther. Sci. 27 (2), 441–445. https://doi.org/10.1589/jpts.27.441.

Heuvelmans, P., Benjaminse, A., Bolt, R., Baumeister, J., Otten, E., Gokeler, A., 2022. Concurrent validation of the Noraxon MyoMotion wearable inertial sensors in change-of-direction and jump-landing tasks. Sports Biomech. 1–16 https://doi.org/10.1080/14763141.2022.2093264.

Kadaba, M.P., Ramakrishnan, H.K., Wooten, M.E., Gainey, J., Gorton, G., Cochran, G.V. B., 1989. Repeatability of kinematic, kinetic, and EMG Data in normal adult gait. J. Orthop. Res. 7 (6), 849–860.

Leppänen, M., Pasanen, K., Kujala, U.M., Vasankari, T., Kannus, P., Äyrämö, S., Krosshaug, T., Bahr, R., Avela, J., Perttunen, J., Parkkari, J., 2017. Stiff landings are associated with increased ACL injury risk in young female basketball and floorball players. Am. J. Sports Med. 45 (2), 386–393. https://doi.org/10.1177/0363546516665810.

Lloyd, D., 2021. The future of in-field sports biomechanics: Wearables plus modelling compute real-time *in vivo* tissue loading to prevent and repair musculoskeletal injuries. Sports Biomech. 1–29 https://doi.org/10.1080/14763141.2021.1959947.

McGinley, J.L., Baker, R., Wolfe, R., Morris, M.E., 2009. The reliability of three-dimensional kinematic gait measurements: A systematic review. Gait Posture 29 (3), 360–369. https://doi.org/10.1016/j.gaitpost.2008.09.003.

Nijmeijer, E.M., Elferink-Gemser, M.T., Otten, E., Benjaminse, A., 2022. Optimal and suboptimal video instructions change movement execution in young talented basketball players. Int. J. Sports Sci. Coach. https://doi.org/10.1177/17479541221118882.

Piazza, S.J., Cavanagh, P.R., 2000. Measurement of the screw-home motion of the knee is sensitive to errors in axis alignment. J. Biomech. 33 (8), 1029–1034. https://doi.org/10.1016/S0021-9290(00)00056-7.

Poitras, I., Dupuis, F., Bielmann, M., Campeau-Lecours, A., Mercier, C., Bouyer, L., Roy, J.-S., 2019. Validity and reliability of wearable sensors for joint angle estimation: A systematic review. Sensors 19 (7), 1555. https://doi.org/10.3390/s19071555.

Reinschmidt, C., van den Bogert, A.J., Lundberg, A., Nigg, B.M., Murphy, N., Stacoff, A., Stano, A., 1997. Tibiofemoral and tibiocalcaneal motion during walking: External vs. skeletal markers. Gait Posture 6 (2), 98–109. https://doi.org/10.1016/S0966-6362(97)01110-7.

Roach, K.E., Miles, T.P., 1991. Normal hip and knee active range of motion: The relationship to age. Phys. Ther. 71 (9), 656–665. https://doi.org/10.1093/ptj/71.9.656.

Robinson, M.A., Sharir, R., Rafeeuddin, R., Vanrenterghem, J., Donnelly, C.J., 2023. The non-sagittal knee moment vector identifies 'at risk' individuals that the knee abduction moment alone does not. Sports Biomech. 22 (1), 80–90. https://doi.org/10.1080/14763141.2021.1903981.

Schepers, M., Giuberti, M., Bellusci, G., 2018. Xsens MVN consistent tracking of human motion using inertial sensing. doi: 10.13140/RG.2.2.22099.07205.

Sinclair, J., Hebron, J., Taylor, P.J., 2015. The test-retest reliability of knee joint center location techniques. J. Appl. Biomech. 31 (2), 117–121. https://doi.org/10.1123/JAB.2013-0312.

Teufl, W., Miezal, M., Taetz, B., Fröhlich, M., Bleser, G., Williams, J.L., 2019. Validity of inertial sensor based 3D joint kinematics of static and dynamic sport and physiotherapy specific movements. PLoS One 14 (2), e0213064.

Vicon Motion Systems, 2016. Vicon Nexus user guide. p. 209. https://docs.vicon.com/display/Nexus25/PDF+downloads+for+Vicon+Nexus.

Windolf, M., Götzen, N., Morlock, M., 2008. Systematic accuracy and precision analysis of video motion capturing systems—Exemplified on the Vicon-460 system. J. Biomech. 41 (12), 2776–2780. https://doi.org/10.1016/j.jbiomech.2008.06.024.

Xsens Technologies B.V., 2021. MVN user manual. https://www.xsens.com/hubfs/Downloads/usermanual/MVN_User_Manual.pdf.

Zarins, B., Rowe, C.R., Harris, B.A., Watkins, M.P., 1983. Rotational motion of the knee*. Am. J. Sports Med. 11 (3), 152–156. https://doi.org/10.1177/036354658301100308.

Zhang, J.-T., Novak, A.C., Brouwer, B., Li, Q., 2013. Concurrent validation of Xsens MVN measurement of lower limb joint angular kinematics. Physiol. Meas. 34 (8), N63–N69. https://doi.org/10.1088/0967-3334/34/8/N63.